**8th World Conference on Experimental Heat**
**Transfer, Fluid Mechanics, and Thermodynamics**
**June 16-20, 2013, Lisbon, Portugal**

# DIGITAL COLOR IMAGE PROCESSING TECHNIQUE APPLIED TO GAS COMBUSTION DIAGNOSTICS

**Teodoro P. Trindade*, João M. Sanches** and Edgar C. Fernandes****

* ISEL – Instituto Superior de Engenharia de Lisboa, Lisbon, 1959-007, Portugal
** IST – Instituto Superior Técnico, Lisbon, 1049-001, Portugal
E-mail: teodoro@deq.isel.ipl.pt

***Keywords*** *: Flame color characterization, Gas premixed combustion, Chemiluminescence.*

## ABSTRACT

The applicability of image data information to estimate the spatial distribution of equivalence ratio at the flame front on gas combustion systems are presented and discussed. The objective is to devise a procedure capable of converting a single RGB image data, obtained by conventional CCD cameras, into a reliable sensing on local combustion state for practical atmospheric flames of premixed methane and propane gases. Flame image information need to be processed and filtered in order to extract representative data whose physical interpretation is usually not straightforward, depending on the transfer function of the instrumentation system. To overcome this issue, is necessary for subsequent analysis to have a experimental reference database of flame images, obtained at controlled camera and combustion conditions. The image sensing signal used in numerical method must exhibit adequate sensitivity to changes in combustion state, otherwise it may entail some information loss. Selecting multiple signals at the same image location enlarges data validation but also increases the computational processing time. Using two camera types, the results obtained over a wide range of practical methane/propane flame conditions ($0.8 \leq \phi \leq 1.4$) are thought to support the applicability of the proposed method for flame diagnostics.

## 1. INTRODUCTION

The radiation emitted by premixed flames of hydrocarbon-based fuels exhibits discrete bands in the visible electromagnetic spectrum (Figure 1) [1]. These bands correspond to the spontaneous light emissions of excited intermediate radicals, formed along the kinetic combustion mechanism, when returning to a lower energy level, such as their ground state. This phenomenon, known as chemiluminescence, is closely related to the combustion state and may be interpreted as a *"signature"* of a particular burning condition. Relevant combustion properties such as flame temperature, heat release rate and pollutant formation, typically depends on the burning conditions reflecting the proximity of the gas mixture to its stoichiometric proportion. A widely used quantification of the mixture stoichiometry is given by the equivalence ratio [2] denoted as $\phi$ and generically defined by Eq.(1).

$$\phi = \frac{(Air - to - Fuel\ Ratio)_{actual}}{(Air - to - Fuel\ Ratio)_{stoichiometric}} \tag{1}$$

A value of $\phi = 1$ corresponds to stoichiometric conditions, at which the reactants molar proportion of fuel to air are well balanced in such that theoretically all combustible species could be completely burned with no oxygen remaining in the products. Values of $\phi > 1$ represent fuel-rich conditions (excess fuel) and $\phi < 1$ fuel-lean conditions (excess air).

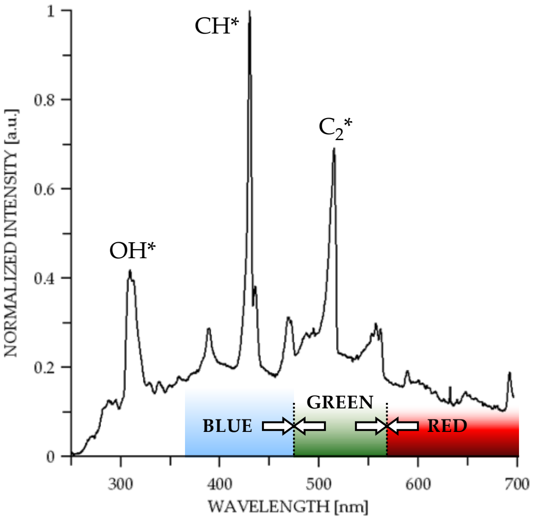

Figure 1: Emission spectrum at near-UV and visible regions of a stoichiometric propane/air premixed flame.

Chemiluminescent flame emissions in the spectrum visible region mainly corresponds to the population distribution of radicals CH* (band head at 430 nm) and $C_2^*$ (Swan system centered on 473 and 515 nm) who's responsible for the blue-green coloration of premixed flames. Herein the symbol * indicates a combined electronic/vibrational/rotational excited level above the ground energy state of the correspondent chemical specie. Varying combustion conditions of premixed reactants ($\phi$), the response of the kinetic oxidation mechanism alters the radical distribution producing changes in the CH* and $C_2^*$ chemiluminescence intensities and thus in the coloration exhibit by flame.

Using spectroscopic techniques, the flame chemiluminescent effect has already been explored to monitor and control a large number of relevant flame parameters [3] such as temperature distribution [4], location of reaction fronts [5] magnitude of local heat release rates [6] or equivalence ratio [7]. The practical relevance of these light related parameters forced the development of novel monitoring techniques [8], in particular involving little demanding instrumentation requirements. In principle, flame images collected using conventional 2D CCD (charge coupled device) cameras covers the data needed requirements in a significant range of combustion conditions [9]. As the RGB photo-sensors responds to visible wavelength and also part of the near-infrared, a color flame image is therefore a combined product correspondent to a broadband radiation of local emissions. Hydrocarbon flame images combines chemiluminescent radiation mainly due to CH*, $C_2^*$ and $CO_2^*$ emitters plus black-body emission from soot particles [10]. The presence of soot on flames has a strong and markedly different dependency on equivalence ratio, degree of premixness and fuel type. In general, emissions from gas flames at $\phi > 1.4$ are dominated by diffusive effects where the black-body radiation is very intense having small chemiluminescence contributions, which restricts the method applicability. Another limitation arises at lean flame conditions where visible chemiluminescent emissions from CH* and $C_2^*$ tends to disappear remaining only the contribution of $CO_2^*$ broad-band, whose intensity is also lowered by the decline of flame temperature. Depending on the vision instrumentation sensitivity to smaller wavelengths, the method loses efficiency on $\phi$ estimate at flame premixture approaching $\phi = 0.8$.

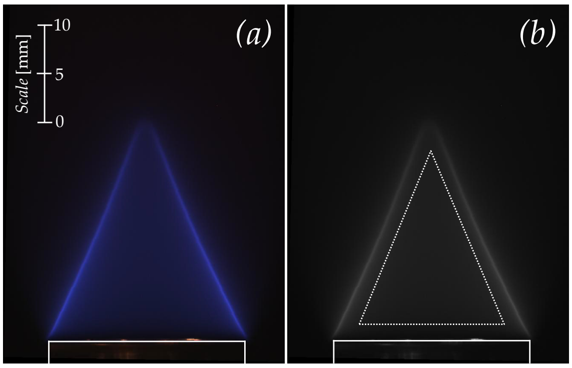

Figure 2: Stoichiometric methane/air premixed flame (1.0 kW): (*a*) raw color image (Jai camera at exposure time: 1000 ms); (*b*) gray-scale image and region of interest (ROI: ····) for color processing methodology.

In the overall process of local equivalence ratio estimate based on RGB data processing, identification of image relevant and usable data is thought to be the main challenge. These image features do not have an intrinsic physical meaning because the transfer function of the overall instrumentation system, relating flame emission characteristics and image intensities, is unknown, serving only as relative indicators of a particular combustion state. Therefore, for practical purpose any attempt to exploit a flame image data involves a previous calibration task using flames at reference conditions for each specific setup of instrumentation hardware. Having a flame image database at different $\phi$ enables a comparison between reference signal combinations, designed here as numerical descriptors (*D*), and the correspondent value in a tested flame image to estimate the unknown burning conditions.

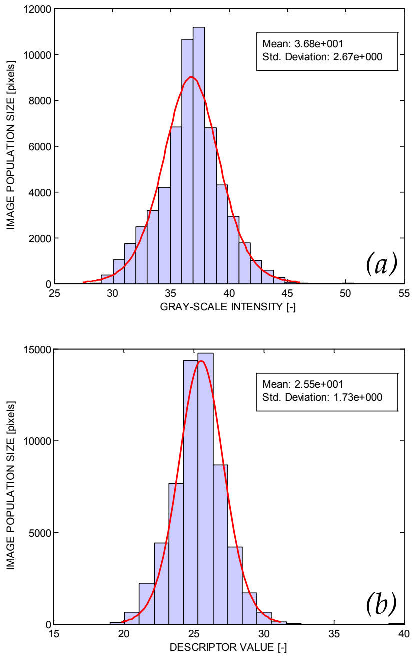

Figure 3: Probability distribution of pixel intensity at the flame front ROI on reference image (stoichiometric $CH_4$/air). Jai camera data at exposure time of 1 s: (*a*) gray-scale intensities; (*b*) green channel intensities.

## 2. EXPERIMENTAL SETUP

A Bunsen-type burner with an outlet diameter of 20 mm was used to generate premixed laminar methane/air and propane/air flames, as calibration references. Uniform gas velocity profiles of the combustion flow at the nozzle outlet were ensured by a higher ratio of contraction areas that equals 25. Fuel and air flows to the burner were measured during the experiments by precision mass flow controllers. High purity methane and propane (≥ 99.95%) supplied in gas cylinders were used as fuels and compressed atmospheric air as oxidizing. Experimental combustion conditions using $CH_4$ and $C_3H_8$ were tested at flame power of 0.75 to 1.75 kW, in a range of equivalence ratios from 0.80 to 1.40. The precision of $\phi$ value in the reference flames where estimate to be in the range of ± 0.01.

In the present study, two imaging systems were used. One representing a conventional equipment, consists on a Reflex Nikon D80 digital CCD color camera (24 bit, 3872×2592 pixels), equipped with a 35:135 mm lens. An alternative image system is a RGB color 3-CCD area scan camera (JAI CV-M9GE) having a resolution of 1024×768 active pixels per color (10 bit). The optics used was a UV/VIS 105 mm CoastalOpt SLR lens, having light transmission efficiencies higher than 85% in the near-UV/Vis range (250-650 nm).

Bayer mosaic color cameras, like the Nikon D80, uses an array pattern of color filters and an interpolation algorithm to estimate the RGB values of each pixel. This results in an averaging of color values to maintain image resolution, producing smoother transitions between adjacent pixels. The overlap of spectral responses for the red ($R$), green ($G$) and blue ($B$) filters also contributes to the uncertainty of some color patterns in this type of equipment. On the other hand, the 3-CCD camera technology uses dichroic prism optics to split incoming light into three separate imagers based on spectral wavelength. Each color channel has the $R$, $G$ and $B$ raw intensity value at full spectral resolution, where no signal interpolation is required. Additionally, the steep spectral response curves resulting from the dichroic prism coating reduce crosstalk between channels, being expected an enlargement of the pixel dynamic range and less color contamination.

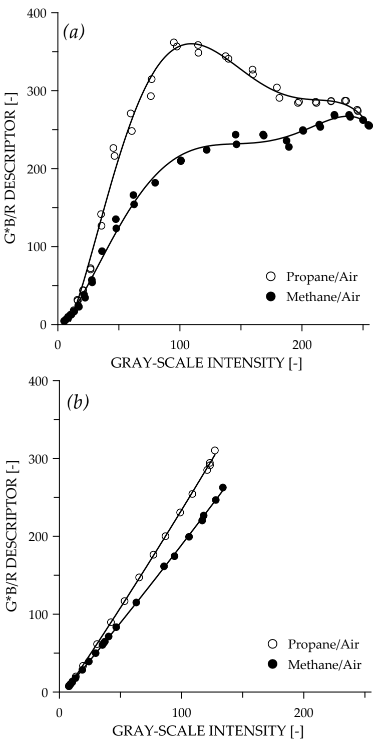

Figure 4: Stoichiometric methane (•) and propane (o) premixed flames image data: (points) experimental, (line) model. Calibration profiles of $G{\cdot}B/R$ descriptor value on average gray-scale intensity using: (*a*) Nikon camera; (*b*) Jai camera.

## 3. RESULTS

It is well known that the color exhibit by an image is, among several other parameters, a function of the camera shutter-speed. Variations in flame power produce the same effect of camera shutter-speed, as they alter intensity and thus the signal distribution between $R$, $G$ and $B$ image channels. Thus, an essential step on digital flame image post-processing must be a normalization procedure to account for intensity variations in the source object. A possible evaluation of pixel intensity can be made forming a weighted sum of the $R$, $G$ and $B$ components ($I$), which corresponds to a gray-scale conversion, Eq.(2).

$$I = r_0\, R + g_0\, G + b_0\, B \tag{2}$$

The coefficients $c_0 = (r_0, g_0, b_0)$ on Eq.(2) can assume any type of weighted proportion, although the values used in the present study was $c_0 = (0.2989, 0.5870, 0.1140)$, which represents the average human perception of colors [11], being substantially more sensitive to green and least sensitive to blue.

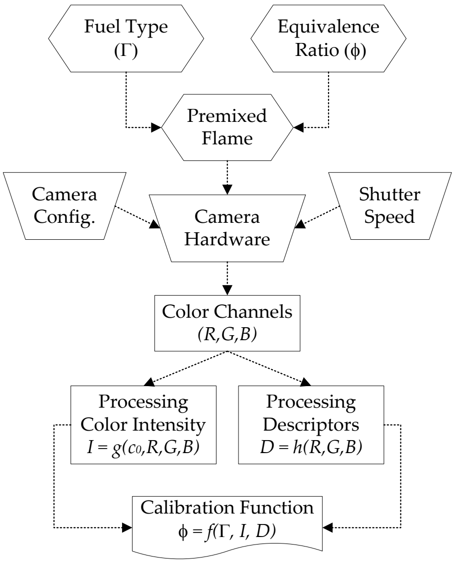

Figure 5: Structure of reference image colection and post-processing procedure by Matlab routines for extracting the flame calibration transfer function.

In order to evaluate the intensity/color relations, reference experimental flame images at different combustion states ($0.80 \leq \phi \leq 1.40$) was experimentally obtained using several camera exposure time, ranging from 2 s to 1 ms. Premixed $CH_4$/air and $C_3H_8$/air Bunsen-type flames (0.75-1.75 kW), was used. All flame images acquired are transferred and post-processed by code routines (MATLAB version 7.10.0 R2010a, The MathWorks Inc., 2010) on a personal computer in order to extract characteristic signal data. Selecting a region of interest (ROI) on each of the reference images, covering the flame front area, Figure 2(b), the intensity (gray-scale, $I$) and color signal numerical descriptors $D$ are computed on every inner pixel. Being the descriptors defined by arbitrary mathematical combinations of $R$ and/or $G$ and/or $B$ values. Typical results of signals density distributions are presented on Figure 3, for gray-scale and $G$ descriptor intensities. Ideally, reference image data should assume a single value, although the experimental dispersion exhibits average standard deviation which can be as high as ± 8%. Processing images at different level of intensity, it is possible to model the dependency between $I$ and each descriptor data. Figure 4 represents experimental calibration data (points) and numerical model (lines) dependency of descriptor $D = G{\cdot}B/R$ on $I$ for premixed propane and methane/air flames at $\phi = 1$.

Extending the procedure to several flame conditions, it is possible to produce of a reference frame relating each descriptor value ($D$), the average intensity ($I$) and the flame state condition ($\phi$), which only depends on fuel type. A diagram that summarizes the image collection and image color processing methodology is presented on Figure 5.

Several descriptors, made by arrangements of $R$, $G$ and $B$ levels, were evaluated by its characteristic profiles against $I$, in order to establish his adequacy on $\phi$ estimate. Figure 6 represents the Nikon camera calibration transfer function of descriptor $D = B/G$, for methane/air (Figure 6a) and propane/air (Figure 6b) premixed flames.

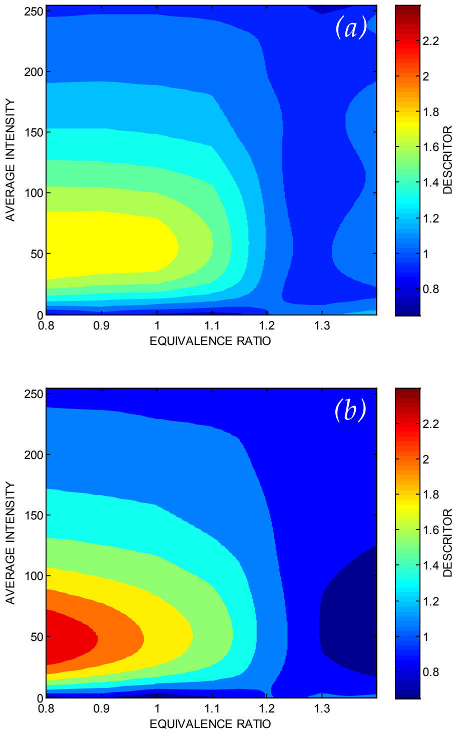

Figure 6: Nikon camera transfer function diagrams of $D = B/G$: ($a$) $CH_4$/air, and ($b$) $C_3H_8$/air flames.

Dark images (low intensity values) and saturated images (higher intensities) are of little interest as the descriptor values exhibits small differences among combustion states. In general, considering Nikon camera data, the gray-scale intensities lower than 20 and higher than 225 have a limited practical use in the detection method. For a given descriptor, the best intensity range on $\phi$ detection depends on their local derivative, i.e. their rate of change with respect to $\phi$ (Figure 7). A specific descriptor $D$ has characteristic regions of interest defining areas having larger values of $\delta D/\delta\phi$, correspondent to higher sensitivities on $\phi$ detection. Considering the descriptor $B/G$ the best detection zone using Nikon camera, roughly corresponds to pixels intensity in the range $25 \leq I \leq 100$, to detect flame equivalence ratios between 1.05 and 1.25 (Figure 7). These regions depends not only on the descriptor type used but also on the sensitivity response of the imaging equipment. Higher signal descriptors amplitudes are obtained by Jai camera when compared with data from Nikon camera. This effect is observed on Figure 8 where a substantially lower and noizy descriptor signal is obtained using the single CCD Nikon camera.

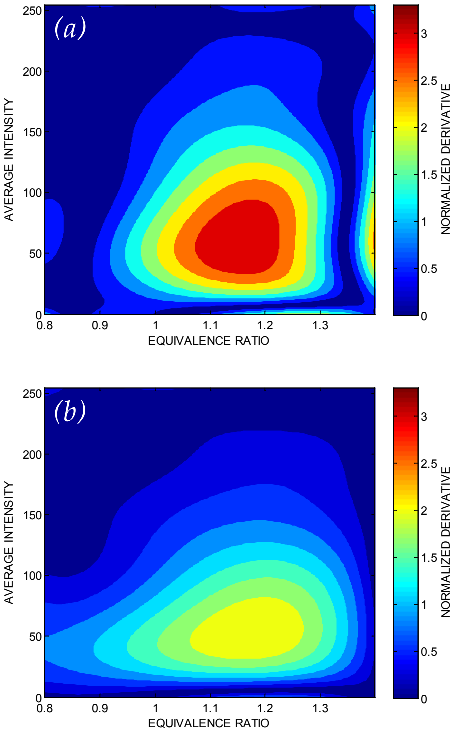

Figure 7: Nikon camera contour maps of $D = B/G$ rate of change ($\delta D/\delta\phi$) for: ($a$) $CH_4$/air, and ($b$) $C_3H_8$/air flames.

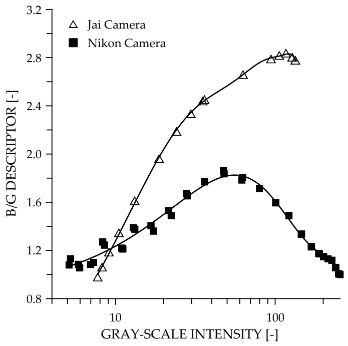

Figure 8: Stoichiometric premixed $CH_4$/air calibration flame data of $B/G$ descriptor collected using Jai (Δ) and Nikon (□) cameras.

In a flame image, like the one presented on Figure 9a, the pixel intensities are not constant having regions of poor detection while others have reasonable intensity. To overcome this problem of anisotropy, the equivalence ratio estimation method should apply over the same image several descriptors, preferably having complementary sensitivity regions.

The image color processing methodology numerically applies over all pixel images the calibration transfer function of each descriptor. The results are several spatial equivalence ratio distributions, one per each of the $N_D$ descriptors. A weighted sum of all computed distributions produces an average map of $\phi$ and represents the model estimates. The weighted method used is a local descriptor rate of change, normalized over all descriptors (Eq.3). This procedure enables an increase of relevance in the predictions made by locally most sensitive descriptors.

$$\phi_{xy} = \frac{\sum_{i=1}^{N_D} \left( \frac{\partial D_i}{\partial \phi} \right)_{\phi_{D_{i,xy}}, I_{xy}} \cdot \phi_{D_{i,xy}}}{\sum_{i=1}^{N_D} \left( \frac{\partial D_i}{\partial \phi} \right)_{\phi_{D_{i,xy}}, I_{xy}}} \tag{3}$$

The numerical image processing technique described before was tested under rich flame conditions on images of a domestic boiler burner (Figure 9a). Their estimation results produce a consistent distribution of $\phi$ along flame front (Figure 9d). Using this method as a diagnostic tool, that can contribute to increase the overall combustion efficiency through improvements in the burner design.

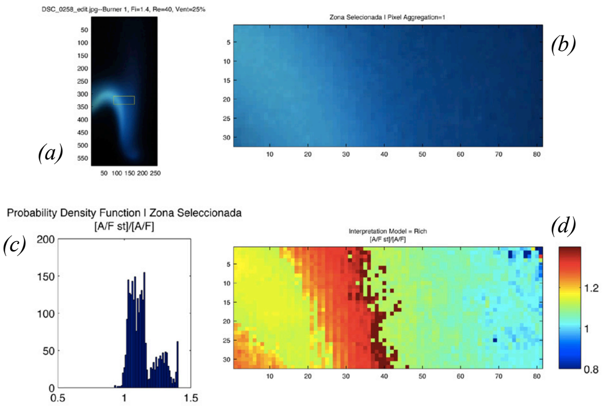

Figure 9: Methane/air flame of a domestic boiler burner ($N_{Reynolds} = 40$): (*a*) Nikon RGB image; (*b*) magnification of a selected region across flame front; (*c*) probability function of $\phi$ on selected region; (*d*) spatial distribution of flame equivalence ratio estimates using 3 descriptors: $B/G$, $G{\cdot}B/R$ and $R/(R+G+B)$.

## 4. CONCLUSIONS

The work presented explore a way to characterize premixed gas flames using embedded information on digital flame images of atmospheric premixed methane/air and propane/air, obtained by conventional CCD cameras, as a diagnostic tool for practical gas combustion applications. The possibility of using RGB color model as a combustion sensor relay on the observation that CH* and $C_2^*$ chemiluminescence emissions are linked particularly to the average values of the *B* and *G* color image channels, at rates dependent on fuel type. The main advantages of using a conventional camera as a flame sensor rely on cost effective, readily available equipment and a possibility to interface with a computer producing a real time 2D distribution with high spatial resolution.

An image database of $CH_4$ and $C_3H_8$ flames was experimentally obtained under strictly controlled conditions, using two different equipment types: a Nikon camera whose RGB images are obtained by a single CCD and Bayer mosaic interpolation scheme, and a 3-CCD Jai camera raw image. A numeric post-processing algorithm, written in MATLAB® and a reference flame image calibration data, was used to compute a set of numerical parameters describing the dependency between the descriptor value (*D*), the gray-scale intensity (*I*) and the flame equivalence ratio ($\phi$), for both gas fuel type tested ($CH_4$ and $C_3H_8$). The application of multiple descriptors to a flame image data enables the estimate of local equivalence ratio distribution along the flame front, roughly in a range of $\phi$ between 0.8 and 1.4.

## REFERENCES

1. A.G. Gaydon, *The Spectroscopy of Flames*, 2nd edition, Chapman & Hall, London, 1974.
2. I. Glassman and R.A. Yetter, *Combustion*, 4th edition, Elsevier, San Diego, 2008.
3. N. Docquier and S. Candel, Combustion Control and Sensors: a Review, *Progress in Energy and Combustion Science,* vol. 28(2), pp. 107-150, 2002.
4. Y. Ikeda, T. Kurahashi, N. Kawahara and E. Tomita, Temperature Measurements of Laminar Propane/Air Premixed Flame Using Detailed OH* Spectra Intensity Ratio, *12th International Symposium on Applications of Laser Techniques to Fluid Mechanics,* Lisbon, 2004.
5. A.F. Ghoniem, S. Park, A. Wachsman, A. Annaswamy, D. Wee and H. Altay, Mechanism of Combustion Dynamics in a Backward-Facing Step Stabilized Premixed Flame, *Proceedings of the Combustion Institute*, vol. 30(2), pp. 1783-1790, 2005.
6. J-R. Kim, Fumiteru Akamatsu, G-M. Choi and D-J. Kim, Observation of Local Heat Release Rate with Changing Combustor Pressure in the CH4/Air Flame (Wrinkled Laminar Regime), *Thermochimica Acta,* vol. 491, pp. 109-115, 2009.
7. M.M. Tripathi, S.R. Krishnan, K.K. Srinivasan, F-Y Yueh and J.P. Singh, Chemiluminescence-Based Multivariate Sensing of Local Equivalence Ratios in Premixed Atmospheric Methane-Air Flames, *Fuel,* vol. 93,

pp. 684-691, 2012.

8. J. Ballester and T. García-Armingol, Diagnostic Techniques for the Monitoring and Control of Practical Flames, *Progress in Energy and Combustion Science,* vol. 36(4), pp. 375-411, 2010.
9. H.W. Huang and Y. Zhang, Digital Colour Image Processing Based Measurement of Premixed CH4 + Air and C2H4 + Air Flame Chemiluminescence, *Fuel,* vol. 90(1), pp. 48-53, 2011.
10. H.W. Huang and Y. Zhang, Flame Colour Characterization in the Visible and Infrared Spectrum using a Digital Camera and Image Processing, *Measurement Science and Technology,* vol. 19(8), 085406, 2008.
11. M. Grundland and N.A. Dodgson, Decolorize: Fast, contrast enhancing, color to grayscale conversion, *Pattern Recognition,* vol. 40, pp. 2891-2896, 2007.